Gene expression and metabolite analysis in barley inoculated with net blotch fungus and plant growth-promoting rhizobacteria

Aurélie Backes, Sophie Charton, Sébastien Planchon, Qassim Esmaeel, Kjell Sergeant, Jean-Francois Hausman, Jenny Renaut, Essaid Ait Barka, Cédric Jacquard, Gea Guerriero

Gene expression and metabolite analysis in barley inoculated with net blotch fungus and plant growth-promoting rhizobacteria

Aurélie Backes [a], Sophie Charton [b], Sébastien Planchon [b], Qassim Esmaeel [a], Kjell Sergeant [c], Jean-Francois Hausman [c], Jenny Renaut [c], Essaid Ait Barka [a], Cédric Jacquard [a], Gea Guerriero [c]

[a] Université de Reims Champagne-Ardenne, RIBP EA4707 USC INRAE 1488, SFR Condorcet FR CNRS 3417, 51100 Reims, France ; aurelie.backes@univ-reims.fr (A.B.) ; qassim.esmaeel@univ-reims.fr (Q.E.) ; ea.barka@univ-reims.fr (E.A.B.)

[b] Luxembourg Institute of Science and Technology (LIST), Environmental Research and Innovation (ERIN) Department, Biotechnologies and Environmental Analytics Platform (BEAP), 41 rue du Brill, L-4422 Belvaux, Luxembourg ; sophie.charton@list.lu (S.C.) ; sebastien.planchon@list.lu (S.P.)

[c] Luxembourg Institute of Science and Technology (LIST), Environmental Research and Innovation (ERIN) Department, GreenTech Innovation Centre, 5 rue Bommel, Z.A.E. Robert Steichen, L-4940 Hautcharage, Luxembourg ; kjell.sergeant@list.lu (K.S.) ; jean-francois.hausman@list.lu (J-F.H.) ; jenny.renaut@list.lu (J.R.)

Corresponding author: gea.guerriero@list.lu (G.G.)
Co-corresponding author: cedric.jacquard@univ-reims.fr (C.J.)

Abstract

Net blotch, caused by the ascomycete *Drechslera teres*, can compromise barley production. Beneficial bacteria strains are of substantial interest as biological agents for plant protection in agriculture. Belonging to the genus *Paraburkholderia*, a bacterium, referred to as strain B25, has been identified as protective for barley against net blotch. The strain *Paraburkholderia phytofirmans* (strain PsJN), which has no effect on the pathogen's growth, has been used as control. In this study, the expression of target genes involved in cell wall-related processes, defense responses, carbohydrate and phenylpropanoid pathways was studied under various conditions (with or without pathogen and/or with or without bacterial strains) at different time-points (0-6-12-48 h). The results show that specific genes were subjected to a circadian regulation and that the expression of most of them increased in barley infected with *D. teres* and/or bacterized with the strain PsJN. On the contrary, a decreased gene expression was observed in the presence of strain B25. To complement and enrich the gene expression analysis, untargeted metabolomics was carried out on the same samples. The data obtained show an increase in the production of lipid compounds in barley in the presence of the pathogen. In addition, the presence of strain B25 leads to a decrease in the production of defense compounds in this crop. The results contribute to advance the knowledge on the mechanisms occurring at the onset of *D. teres* infection and in the presence of a biocontrol agent limiting the severity of net blotch in barley.

Additional keywords: Barley, Biocontrol, *Drechslera teres*, Beneficial bacteria, RT-qPCR, Metabolomics.

1. Introduction

Barley (*Hordeum vulgare* L.) is one of the most important cereal crops cultivated in the world (Ferdous et al., 2015). Due to its worldwide distribution and use, barley has a significant economic impact. Caused by an ascomycete, *Drechslera teres*, net blotch is the foliar disease resulting in the most severe damages on barley (Backes et al., 2021a). It is a disease whose symptoms quickly appear in the form of dark spots. These spots will then enlarge to give way to necrotic lesions followed by a chlorotic halo around the zone of penetration. The disease is responsible for an important loss in barley yields (up to 40%) in different cultivation areas and represents a serious threat for the brewing sector.

The use of plant growth-promoting rhizobacteria (PGPR) to induce the plant resistance is one of the alternatives considered to protect crops against the damage caused by cryptogamic diseases (Prasad et al., 2019). *Paraburkholderia phytofirmans* strain PsJN, a well-known PGPR, has been isolated from surface-sterilized onion roots (Nowak, 1998). PsJN is able to colonize a large variety of plants, such as tomato, potato and grapevine. In addition, this bacterium improves the tolerance against biotic stress (Miotto-Vilanova et al., 2016). According to previous results, PsJN has no antagonistic effect against *D. teres* in barley (Backes et al., 2020). Therefore, this bacterium was used as a bacterization control in this study. Unlike PsJN, another bacterium, belonging to the genus *Paraburkholderia* was able to limit significantly the development of *D. teres*. This is a new species of *Burkholderia* after a comparison against all genomes of typical strains available in the Microbial Genomes Atlas (MiGA) webserver and TYGS database. Therefore, *Paraburkholderia* sp. is the name proposed for the beneficial bacterium having an antagonist effect against net blotch and referred to as strain B25 in the present investigation.

Biotic stresses induce physiologic, transcriptomic and metabolomic changes in plants. The different experiments discussed in this present study were designed with the goal of improving the knowledge about the changes induced at the genes' and metabolites' level after infection by *D. teres* and application of beneficial bacteria on barley.

When the pathogen attacks the plant, defense mechanisms are quickly activated. More particularly, barley-pathogen interactions can lead to compatible response (infection) or incompatible (resistance). In the case of infection, pathogens elicit a set of localized responses around the site of infection. Oxidative burst is one of the early responses, which generally leads to programmed cell death through the hypersensitive response (HR). Reactive oxygen species (ROS) contribute to oxidative stress and have a toxic effect in plants and field crops. Barley has developed protective mechanisms to counteract oxidative stress: among them, glutathione *S*-transferase (*GST*), superoxide dismutase (*SOD*) and catalase *(CAT*) are well-known antioxidant enzymes (Lightfoot et al., 2017). Phytohormones, such as jasmonic acid (JA), also play a major role in the signaling networks involved in plant responses to biotic stress. Studies have shown the enhanced synthesis of this phytohormone during fungal pathogens' attack (Qi et al., 2016). Additionally, cereals activate systemic defense responses in uninfected plant parts in parallel with local reactions. These reactions involve pathogenesis-related (*PR*) genes, which enhance the resistance to infection.

The plant cell wall is a dynamic and complex structure and represents the first physical barrier against pathogens (including virus, bacteria, fungi, nematodes and other pests). The cell wall is composed of a network of cellulosic and non-cellulosic polysaccharides, which can be impregnated by the hydrophobic aromatic polymer lignin (Yadav et al., 2020). The plant cell wall is constantly

involved in interactions between plants and their environment: for instance, the cell wall composition and structure change to limit the further spread of fungal pathogens.

Moreover, enzymes belonging to the phenylpropanoid biosynthetic pathway are involved in the changes in cell wall composition and in the production of antimicrobial compounds in response to attacks by different pathogens. In plants, the phenylpropanoid pathway is a rich source of metabolites derived from phenylalanine. This pathway is required for the biosynthesis of lignin and serves as a starting point for the production of many other important compounds, such as flavonoids, coumarins and lignans. Many biotic stress-induced phenylpropanoids are classified as phytoalexins. They include isoflavanes, stilbenes, flavonols (e.g. quercetin, kaempferol) and coumarins (Yadav et al., 2020). The levels of these compounds increase around the site of infection to concentrations that are toxic to pathogens (virus, bacteria, fungi, nematodes and other pests) in infected plants. Being a leaf disease, net blotch also negatively affects the physiology of barley and notably photosynthesis (Backes et al., 2021b).

To decipher the physiological and molecular responses of barley inoculated with *D. teres* in the presence and absence of beneficial bacteria, we here aimed to reveal the mechanisms established at two levels: gene expression and metabolites' production. In order to better understand the interaction among barley, *D. teres* and bacteria, we analyzed genes involved in defense (*GST*, *SOD*, *CAT*, *PR8* and *AOC*), in the phenylpropanoid (*PAL*, *CHS* and *F3'H*) as well as carbohydrate pathways (*SUS2*, *RcaA2*) and in cell wall biosynthesis (*GSL* and *CSLF6*). Metabolomic was previously applied to different pathosystems and provided valuable information about the plant/pathogen interaction and allowed the identification of compounds playing a major role in plant innate immunity. Consequently, we combined targeted gene expression analysis to metabolomics to identify similarities or differences in gene transcript levels and metabolic pathways in barley inoculated with *D. teres* in the presence or absence of beneficial bacteria.

2. Materials and Methods

2.1 Plant material, growth conditions and treatments

The cultivar Siberia is a six-row winter barley, which is the most susceptible to net blotch and was therefore chosen to perform the experiments in this study. Barley seedlings were grown in controlled conditions in incubators (Aralab, Portugal) following a cycle of 23 °C day / 22 °C night, 80 % relative humidity, 14 h/10 h day/night photoperiod. Barley seeds were sown in Gramo Flor non-sterile soil without any treatment. A bacterial suspension (strain B25 and PsJN) in PBS at a concentration of 10^9 bacteria/mL was sprayed on the barley plants leaves at stages 11-12 according to the Zadoks scale. In parallel, for the control condition, barley leaves were sprayed only with PBS solution. Three days later, spores of the *D. teres* pathogen diluted in sterile water were also sprayed on barley leaves at a concentration of 4 000 spores/mL. At the same time, control barley plants without *D. teres* were sprayed with sterile water. Sampling of barley plants leaves at stages 12-13 according to the Zadoks scale took place at the following time points: 0, 6 h, 12 h and 48 h post-infection (hpi). Samples from four biological replicates per treatment were obtained and each sample was a pool of 12 plants.

2.2 RNA extraction and cDNA synthesis

Barley leaves were crushed to a fine powder in liquid nitrogen using a mortar and a pestle. Seventy-five mg of finely-ground material were weighed and total RNA was isolated using the TRIzol reagent (Extract'All, Eurobio), according to the manufacturer's instructions. RNA concentration and purity were determined using a Nanodrop ND-1000 spectrophotometer (Thermo Scientific, Villebon-sur-Yvette, France). All RNA samples had an A260/230 ratio between 1.8 to 2.0 and an A260/280 ratio of approximately 2.0. RNA integrity was checked with a Bioanalyzer (Agilent, Santa Clara, CA, USA). All RNAs displayed a RIN above 7. One microgram of RNA was retro-transcribed using the SuperScript II cDNA Synthesis kit (Invitrogen), following the manufacturer's instructions.

2.3 Choice of reference genes, target genes and primer design

Eight reference genes were selected: elongation factor 1 *EF1* (AJ277799.1), glyceraldehyde-3-phosphate dehydrogenase *GAPDH* (AK359500.1), actin *Act* (AY145451.1), ribosomal protein S4 *RP_S4* (NC_042692.1), ubiquitin *UBC* (AK248472.1), ubiquitin *UBC 9* (AK249228.1), cyclophilin *CYP* (AK253120.1) and *S*-adenosyl-L-methionine-dependent methyltransferase superfamily protein *SALM* (AK355689.1).

The target genes chosen are: phenylalanine ammonia lyases *PAL* and *PAL2* (BAJ88975.1 and Z49145.1), glucan synthases *GSL1* and *GSL3* (AY177665.1 and FJ853601.1), chalcone synthase *CHS* (X58339.1), flavonoid 3'-hydroxylase *F3'H* (AK363912.1), cellulose synthase-like gene *CslF6* (AB621305.1), glutathione *S*-transferase d2 *GSTd2* (BAJ99765.1), cytosolic superoxide dismutase *SOD* (KU179438.1), pathogenesis-related protein 8 *PR8* (KAE8773798.1), allene oxide cyclase *AOC* (CAC83766.1), catalase *CAT2* (AAC17730.1), sucrose synthase *SUS2* (CAZ65725.1) and RuBisCO activase *RcaA2* (M55447.1).

Primers were designed using Primer3Plus (http://www.bioinformatics.nl/cgi-bin/primer3plus.cgi) and checked using the OligoAnalyzer 3.1 tool from Integrated DNA technologies (http://eu.idtdna.com/calc/analyzer). Primer efficiencies were determined by RT-qPCR using six serial dilutions of cDNA (10, 2, 0.4, 0.08, 0.016, 0.0032 ng/µL). The list of reference and targeted genes is given in Table 1 with the primer sequences, amplicons' length, melting temperature and primer efficiency.

2.4 Quantitative real-time PCR and statistical analysis

For the RT-qPCR analysis, reactions were performed in 384-well plates using a liquid handling robot (epMotion 5073, Eppendorf, Hamburg, Germany). The cDNA was amplified using the Low Rox SYBR MasterMix dTTP Blue Kit (Eurogentec, Liège, Belgium). The RT-qPCR reactions were set up and run according to Backes et al. (2020) in technical triplicates and repeated on four independent biological replicates on a ViiA 7 Real PCR System (Thermo Scientific, Villebon-sur-Yvette, France). A melt curve analysis was performed at the end to check the specificity of the amplified products. Genes expression was calculated using qBasePLUS (version 3.2, Biogazelle, Zwijnaarde, Belgium). *Act* and *RP_S4* were identified as the most stable genes and as sufficient for normalization in the experimental set up chosen.

161 **Table 1**. List of primers used in the study with details on the amplicons' length, Tm (°C), PCR
162 amplification efficiency (in %) and regression coefficient.

Name	Sequence (5'->3')	Amplicon Length (bp)	Amplicon Tm (°C)	PCR Amplification Efficiency (%)	Regression Coefficient (R^2)
Act Fwd	GGAATCCACGAGACGACCTACA	130	82.7	90.6	0.996
Act Rev	CTTGCTCATACGGTCAGCGATA				
EF1 Fwd	ATGGCATCAAGAAGCTCCAG	131	82.7	99.6	0.989
EF1 Rev	GAAGGCAACAATGTCACAGC				
GADPH Fwd	TGAGGGTTTGATGACCACTG	122	83.9	92.1	0.992
GADPH Rev	CAGTGCTGCTTGGAATGATG				
RP_S4 Fwd	CGATTGGGTATGGCTTCAAC	107	80.0	89.8	0.998
RP_S4 Rev	GGTTTGCAACGAAAACTTGG				
UBC Fwd	TCAATTCCCGAGCAGTATCC	101	81.1	97.2	0.991
UBC Rev	TCCAGGCATATTTCACCAGTC				
CYP Fwd	GCTCCCAGTTCTTCATCTGC	112	87.0	102.4	0.992
CYP Rev	CCCACCTTCTCGATGTTCTT				
UBC9 Fwd	TGCTCCTTTCAATCTGCTCTC	110	85.0	102.5	0.994
UBC9 Rev	CGCTGTGGACTCATACTTCG				
SALM Fwd	GGGAGATTGGCTCTGGAAAT	110	79.0	104.8	0.969
SALM Rev	GCCTCTTGGGTGTGGTTTAG				
PAL Fwd	ACAATGGTCTGCCTTCCAAC	113	86.0	107.8	0.962
PAL Rev	CCCCAAGAATTGAAGCTCAG				
GSTd2 Fwd	GTCGGAAGGTGAAAGAAACG	131	83.0	101.0	0.997
GSTd2 Rev	ATCAAGGTCCAGGACGGATAC				
PR8 Fwd	ACAACAAGGTGAACGGGAAG	100	85.7	95.3	0.991
PR8 Rev	CAGTCCGACACGATGTATCC				
AOC Fwd	ATGTACTTCGGCGACTACGG	146	88.5	103.7	0.997
AOC Rev	TTGAAGGGGAAGACGATCTG				
CAT2 Fwd	TCTTCAACGAGAACGAGCAG	149	89.5	89.9	0.992
CAT2 Rev	GGGGAGCATCAGGTAGTTTG				
GSL1 Fwd	ATTGGATATGGCTGGTCTGG	126	82.9	93.8	0.985
GSL1 Rev	TTCCCTTCACCTTTCTGCAC				
GSL3 Fwd	CAGGGGCTTTGTTGTCTTTC	138	82.9	101.4	0.985
GSL3 Rev	ATGGTCGAGTGGGAAGTTTG				
CHS Fwd	TGGAACTCCGTCTTCTGGATAG	141	88.0	92.7	0.997
CHS Rev	ACATGCACTGGACATGTTGC				
F3'H Fwd	GCCAGGGAGTTCAAGGACA	168	90.4	86.0	0.942
F3'H Rev	CTCGCTGATGAATCCGTCCA				
PAL2 Fwd	AGAAAATGCGTGCGGTTC	82	85.7	110.3	0.990
PAL2 Rev	TTGGCAAACACTGACGTCTC				
CslF6 Fwd	CCGTGCTCTACATCAACATCC	92	83.9	98.1	0.988
CslF6 Rev	TGTGTCGACCAACTTCTTGC				
SOD Fwd	TGACCTCGGAAATGTGACAG	142	84	89.5	0.996
SOD Rev	ACCCTTGCCAAGATCATCAG				
SUS2 Fwd	ACGAACTCAACGTCGAACAG	127	85.7	90.6	0.990
SUS2 Rev	GGGATTAAGGCAGTGAATGG				
RcaA2 Fwd	ACACCGTCAACAACCAGATG	142	86.5	89.6	0.984
RcaA2 Rev	AGCGTCGAGAAATCGTTACC				

163

164

Statistics were performed on log2 transformed data using a one-way ANOVA with a Tukey's post-hoc test after having checked the normal distribution of the data and homogeneity with a Shapiro-Wilk's and a Levene's tests, respectively, using IBM SPSS Statistics V19 (IBM SPSS, Chicago, IL, USA). A hierarchical clustering using uncentered absolute correlation and complete linkage was used to generate groups with similar expression patterns in Cluster 3.0 (correlation coefficient threshold = 0.83). The heat map was visualized with Java TreeView available at http://jtreeview.sourceforge.net/.

The principal component analysis (PCA) was performed with ClustVis (available online at https://biit.cs.ut.ee/clustvis/). To visualize the expression pattern of genes related to the phenylpropanoid and cell wall biosynthetic pathways, the barley eFP Browser (http://bar.utoronto.ca/efpbarley/cgi-bin/efpWeb.cgi) was queried. To obtain the contig number necessary as input in the eFP Browser, the FASTA sequence of the gene was blasted on PLEXdb (Plant Expression Database; http://www.plexdb.org). The expression levels of the genes are shown as a heatmap with yellow and red colors indicating low and high expression, respectively, in various tissues.

2.5 Metabolites extraction and analysis

2.5.1 Freeze-drying and weighing

Metabolomics was performed on the samples corresponding to 12 hpi and 48 hpi. Three biological replicates were analyzed. Samples ground to fine powder were freeze-dried during 48 h. Then, 10 ± 0.2 mg of freeze-dried plant material were weighed and stored at -80 °C until extraction.

2.5.2 Extraction

Leaf samples were extracted with 998 µL of methanol/water (4:1, v/v) and 2 µL of chloramphenicol at 5 mg/mL as internal standard (Sigma-Aldrich). This mixture was homogenized using a vortex during 1 min, and shaken during 4 h at 14 000 rpm and room temperature in a Thermomixer (Eppendorf, Hamburg, Germany), then vortexed again during 30 sec. After centrifugation at 20 000 g for 30 min at 4 °C, 750 µL of supernatant were collected and evaporated to dryness under a nitrogen flow (TurboVapLV, Biotage, Sweden). Samples were resuspended in 375 µL of methanol: water (5:95, v/v) and filtered through 0.22 µm PTFE syringe filter (Millex-LG, Merck KGaA, Darmstadt, Germany).

2.5.3 Untargeted metabolomics analysis with UHPLC-DAD-ESI-MS/MS

Extracts were analyzed using an Acquity UPLC I-class ultra-high pressure liquid chromatography (UHPLC) system equipped with a diode array detector (DAD) (Waters, Milford, MA, USA) coupled to a hybrid quadrupole-time of flight mass spectrometer (TripleTOF 6600, SCIEX, Framingham, MA, USA) in positive and negative ionization modes. Five µL of the samples in random order were separated on a reverse-phase Acquity UPLC BEH C18 column (2.1 x 100 mm, 1.7 µm particle size) (Waters, Milford, MA, USA). The eluents were 0.1 % (v/v) formic acid in water (A) and 0.1 % (v/v) formic acid in acetonitrile (B). The gradient was as follows: 0 min, 1 % B; 4 min, 1 % B; 16 min, 5 % B; 35 min, 40 % B; 45 min, 100 % B; 50 min, 100 % B; 54 min, 1 % B; 60 min, 1 % B. The flow rate was 0.5 mL/min and the column temperature was set to 50 °C. UV-visible spectra were also acquired between 190 and 800 nm at a rate of 10 points/sec.

Electrospray ionization (ESI) was performed on analytes using the following parameter values for positive and negative modes: source temperature 650 °C; ion spray voltage of 4.5 and -4.5 kV, respectively, curtain gas (nitrogen) of 30 psi, nebulizer gas (air) of 55 psi and turbine gas (air) of 50 psi. The declustering potential was set up at 60 V and -60 V in positive and negative mode, respectively. The precursor charge state selection was set at 1. For information-dependent acquisition in high sensitivity mode, survey scans were acquired in 175 msec. In addition, the 10 most abundant products ion scans were collected during 200 msec if exceeding a threshold of 100 counts/sec, thus leading to a total cycle time of 2.225 sec. A sweeping collision energy of 15 V below and above 15 and -15 V, for the positive and negative modes, respectively, was applied to all precursor ions. The dynamic exclusion was set for two seconds after three occurrences before the precursor could be fragmented again. Full high-resolution MS spectra were recorded between 100 and 2000 mass-to-charge ratio (*m/z*) for MS1, whereas MS2 scans were recorded between 50 and 2000 *m/z*, in profile mode.

2.5.4 Data processing and statistical analysis

Data were processed using Progenesis QI (v 2.3, Nonlinear Dynamics, Waters, Newcastle, UK). Briefly, the software automatically extracts features (combinations of isotopic peaks and adducts ions at a given retention time) between 0 and 50 min and aligns them. A normalization to all compounds was carried out. For each comparison of modalities two by two, only features with MS2 data and both fold-change above 1.5 and *p*-value below 0.05 in Progenesis's ANOVA were kept for the identification step, which consisted in the use of Metascope, ChemSpider and National Institute of Standards and Technology (NIST) plugins, for the search in an in-house database, in CHEBI 3-star, in MassBank for the first plugin, in PubChem for the second and in NIST MS/MS database for the third. A manual review of the output data was then carried out, in combination with the software PeakView (v 1.2, SCIEX, Framingham, MA), LipidMaps (http://www.lipidmaps.org/), Metlin (https://metlin.scripps.edu/index.php), MassBank of North America (MoNA) (https://mona.fiehnlab.ucdavis.edu/) and PubChem databases (https://pubchem.ncbi.nlm.nih.gov), as well as literature data for structure elucidation.

To reduce the number of compounds to be identified and further sharpen the analysis, different comparisons were made according to several variables. Indeed, comparisons 1 to 6 were focused on time as variable (12 hpi *vs* 48 hpi), while comparisons from 15 to 20 were dedicated to the pathogen's absence or presence as variable. Finally, only comparisons from 7 to 14, with the presence of either bacteria B25 or PsJN as variable, were further investigated for this study, since we were interested in knowing the effects on barley metabolism of these bacteria used as a biocontrol agent. More specifically, comparisons from 7 to 14 consisted in: control *vs* strain B25 without pathogen at 12 hpi (comparison 7), control *vs* strain B25 with pathogen at 12 hpi (comparison 8), control *vs* strain B25 without pathogen at 48 hpi (comparison 9), control *vs* strain B25 with pathogen at 48 hpi (comparison 10), control *vs* strain PsJN without pathogen at 12 hpi (comparison 11), control *vs* PsJN strain with pathogen at 12 hpi (comparison 12), control *vs* PsJN strain without pathogen at 48 hpi (comparison 13), control *vs* PsJN strain with pathogen 48 hpi (comparison 14).

Annotations and identifications were classified in accordance with the levels of the Metabolomics Standards Initiative (MSI), as described in Sumner et al. (2007). Compounds in class 2 were identified based on exact mass, retention time, MS2 fragmentation pattern and UV-visible spectrum by comparison with data in databases and/or literature. Class 3 was assigned to

compounds with the same information as class 2 when they allowed only chemical class determination, typically when the molecule identified is a fragment of a bigger, not fully determined molecule. Class 4 was allocated to compounds for which only a part of the molecule is elucidated, with no complete molecular formula generated.

3. Results and Discussion

3.1. Gene expression depends on the circadian rhythm and the experimental conditions

As a first step towards understanding the molecular effects of *D. teres* infection and PGPR application on barley leaves, the expression of a selection of genes was analyzed. We performed an *in silico* analysis of the expression values across barley tissues at different developmental time-points, by searching the barley eFP Browser. The goal was to verify that the selected genes were expressed in the leaves.

Genes involved in stress response [glutathione *S*-transferase d2 (*GSTd2*), pathogenesis-related protein 8 (*PR8*), allene oxide cyclase (*AOC*), catalase 2 (*CAT2*), cytosolic superoxide dismutase (*SOD*)], cell wall biosynthesis [glucan synthases (*GSL1* and *GSL3*), cellulose synthase-like (*CslF6*)], carbohydrate metabolism [sucrose synthase 2 (*SUS2*), RuBisCO activase (*RcaA2*)] and the phenylpropanoid pathway [phenylalanine ammonia lyases (*PAL* and *PAL2*), chalcone synthase (*CHS*), flavonoid 3'-hydroxylase (*F3'H*)] were selected, as they provide information on the changes occurring in pathways activated at the onset of biotic stress. Hereafter, we will present the results of a PCA to provide an overview of the data clustering in the experimental conditions and the different time-points studied. We will then report and discuss the expression data for all the genes analyzed.

According to the PCA, four groups, corresponding to the different time-points are visible (Figure 1). The first includes barley plants sampled at T0 (red color). This sampling time corresponds to the start of the day with a light intensity from 0 to 75 %. The second group includes samples taken at 6 hpi (purple color, corresponding to midday, i.e. 75 % light intensity). The third group includes leaves sampled 12 hpi and corresponding to the end of the day with a light intensity decreasing from 75 to 0 % (blue color). The last group includes barley leaves sampled 48 hpi and corresponding again to the start of the day (green color). The distinction of these groups is mainly due to the sampling time-points. A clear grouping of the samples following the time points is evident, hence denoting a dependence on the circadian rhythm (Figure 1). Light affects the host response, as well as the virulence of the bacterial and fungal pathogens. Recent reports have shown direct light effects on the defense response in the host plant. One of the earliest studies providing indications about a connection between circadian rhythm and defense responses was on a pathogen-responsive gene coding for a glycine rich protein (GRP) in barley. Two GRPs (*Hvgrp2* and *Hvgrp3*) were previously shown to be rapidly induced upon fungal pathogens' attack (Sharma and Bhatt, 2015). Defense genes show a peak in expression at midnight and at dawn, the time points coinciding with the time of sporulation and spore dissemination, respectively (Sharma and Bhatt, 2015). Subsequently, other studies have shown modulations of some genes with the circadian cycle (Luna et al., 2005; Dao et al., 2011; Khan et al., 2010). For instance, the level of a catalase-*CAT1* transcript was regulated by the circadian clock and persisted in continuous darkness, whereas *CAT2* expression decreased by night in wheat (Luna et al., 2005). In *Arabidopsis, CHS* expression was also regulated by the circadian clock (Dao et al., 2011). Several enzymes involved in cell wall biosynthesis were found to be regulated by

the circadian rhythm in maize (Khan et al., 2010). To achieve cell wall stiffening, cinnamoyl-CoA reductase (CCR) and cinnamyl alcohol dehydrogenase (CAD) catalyze the final steps in the phenylpropanoid pathway; results have demonstrated that transcripts encoding both enzymes have cyclic expression, peaking at dawn in maize (Khan et al., 2010).

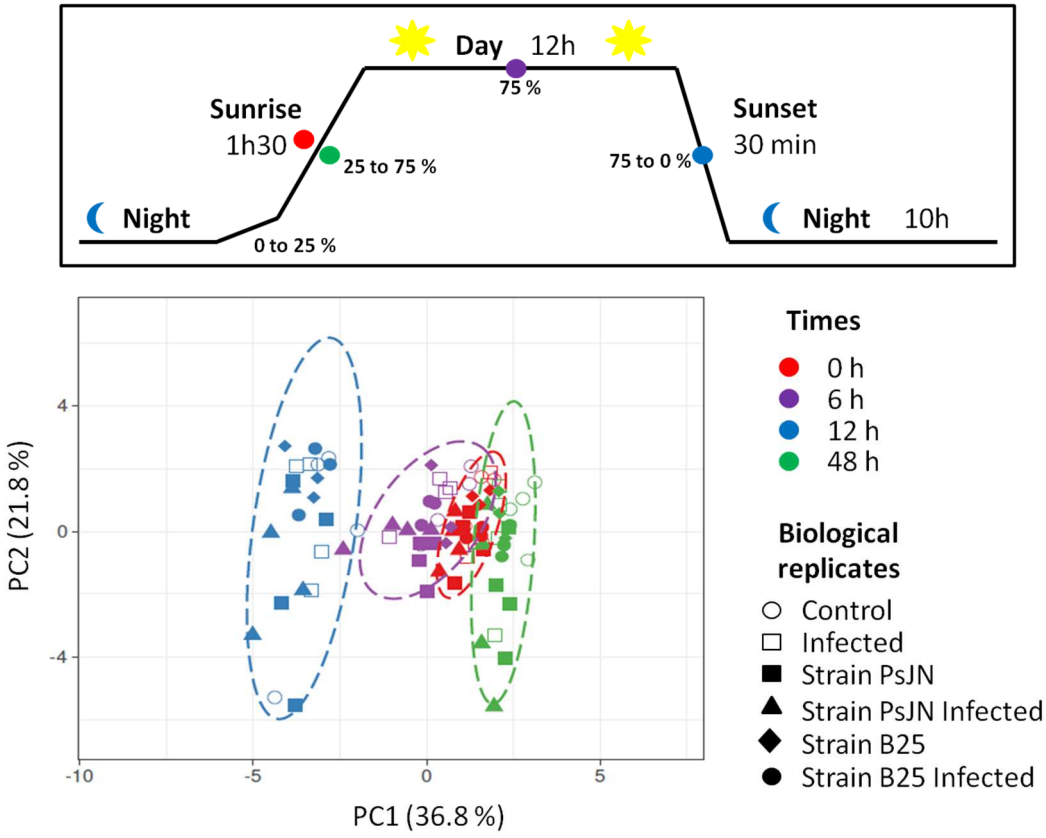

Figure 1. Principal component analysis of the gene expression data. The data are log2-transformed and correspond to the sampling time-points. Four biological replicates are used under the different experimental conditions.

3.2. Gene expression analysis in *D. teres*-infected barley leaves in the absence/presence of PGPR

We will hereafter report the gene expression results by presenting first the changes triggered by *D. teres* and then by focusing on the effects of PGPR addition.

According to the heat map hierarchical clustering (Figure 2), three different expression patterns can be identified in response to *D. teres*. The first group is composed by *PAL2*, *RcaA2*, *PR8*, *SUS2*, *PAL*, *CslF6* and *CHS* and shows no significant variation in gene expression under the experimental conditions. The second group, comprising *GSTd2*, *SOD*, *GSL1*, *GSL3*, *AOC* and *CAT2*, shows a tendency towards an increase at 6 hpi and 12 hpi (Suppl. Table 1). The last group consists only of *F3'H*, which shows a higher expression in the presence of *D. teres* at 12 hpi and 48 hpi. The expression level of this gene is dependent on the sampling time-points. Indeed, its expression tends to increase at 12 hpi and 48 hpi with *D. teres*. In addition, *F3'H* is repressed at 6 hpi, regardless of the experimental condition. On the other hand, the expression of *F3'H* is modulated according to the experimental condition. For example, this is clearly visible at 48 hpi when its expression increases.

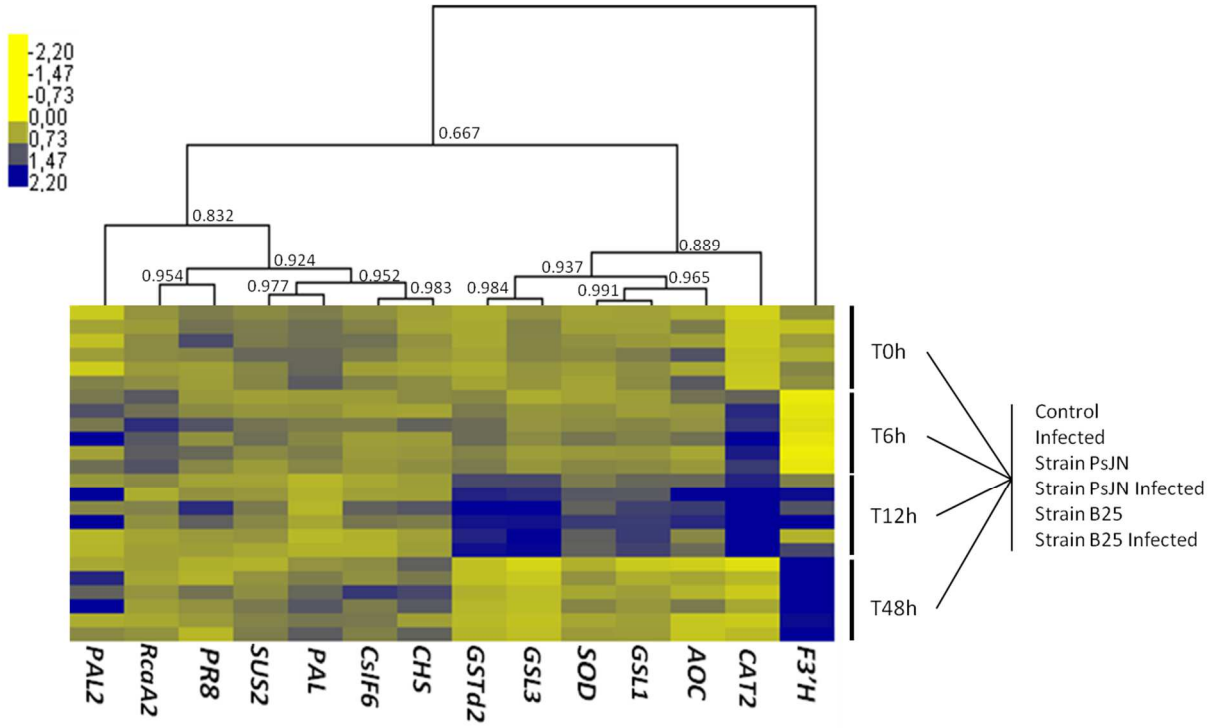

312

313 **Figure 2.** Heatmap hierarchical clustering of genes related to cell wall biosynthesis, defense response,
314 carbohydrate and phenylpropanoid pathway in *H. vulgare* in the absence/presence of the pathogen
315 and/or in combination with strain PsJN or strain B25. The lines refer to the order of the six
316 experimental conditions for each time point. The heat map hierarchical clustering was generated
317 using a Pearson's correlation in complete linkage (the numbers close to the branches indicate the
318 coefficients). The normalized relative quantities and statistics are indicated in Suppl. Table 1.

319 The interaction between plant and different pathogens induces an accumulation of ROS and
320 therefore the expression of genes coding for antioxidant enzymes, such as CAT2, GST and SOD. In the
321 presence of *D. teres* (6, 12 and 48 hpi), the transcripts encoding the antioxidant enzymes CAT2 and
322 GSTd2 have a higher expression compared to *SOD*. The attack of the insect *Nilaparvata lugens* on
323 rice, another monocot, resulted in increased *CAT* and *GST* expression, while *SOD* gene was repressed
324 (Jannoey et al., 2017). According to Lightfoot et al. (2017), *HvCSD1*, a cytosolic *SOD*, was up-regulated
325 during the interaction between barley and the pathogen causing net blotch.

326 Jasmonic acid is a phytohormone synthesized from lipids through the actions of several
327 enzymes including AOC during the acclimation to biotic stresses. At 12 hpi, *AOC* shows a higher
328 expression in the presence of *D. teres* in barley (Figure 2). The difference is not statistically significant
329 (Suppl. Table 1), but it indicates a tendency in the gene expression pattern. According to Maucher et
330 al. (2004), the same result was reported in barley infected with the powdery mildew agent.

331 In this study, *GSL*s and *CslF6* were chosen for their roles in callose deposition and mixed-
332 linkage β-glucan synthesis, respectively. Our results show that *CslF6* does not vary significantly in
333 expression in the presence of the pathogen (Suppl. Table 1). On the contrary, *GSL1* and *GSL3* have a
334 slight increase in expression at 12 hpi in the presence of *D. teres*. Similar results were obtained by
335 Singla et al. (2020), indicating that the β-glucan levels are maintained in barley infected with
336 *Puccinia*.

The genes coding for enzymes belonging to the phenylpropanoid pathway, namely *PAL* and *F3'H*, modulate their expression in the presence of the pathogen (Huang et al., 2010). Phenylalanine ammonia lyase (PAL) catalyzes the deamination of phenylalanine to produce *trans*-cinnamate, which is the first step in the phenylpropanoid pathway. Several studies have shown that *PAL* gene expression is responsive to a variety of environmental stimuli, including pathogen infection by viruses, bacteria, fungi, nematodes and other biotic stressors. Flavonoids, including anthocyanins, flavones and flavonols are ubiquitous secondary metabolites of plants. From a biological perspective, flavonoid biosynthesis plays important roles in the plant's defense against various biotic stresses. Our results show that the expression of *PAL* increases from 12 hpi only in the presence of the pathogen. Comparable results were published during a barley - *Erysiphe graminis* interaction, showing an increase in *PAL* expression at 6 hpi and between 12 hpi and 15 hpi (Shiraishi et al., 1995). In the same way, an increase in *PAL* gene expression was demonstrated 6 hpi by *Blumeria graminis* in barley (Jawhar et al., 2017). A recent RT-qPCR analysis showed an increase in *PAL* expression 6 hpi with *D. teres* in barley, which is in agreement with our results (Arabi et al., 2020).

Two genes involved in photosynthesis were also investigated: RuBisCO activase (*RcaA2*) and sucrose synthase (*SUS2*). During a compatible host-fungal pathogen interaction, like barley and *D. graminea*, RuBisCO activity declined 2 hpi (Goel and Kumar Paul, 2020). Therefore, the pathogen can directly affect photosynthetic mechanisms by affecting the host tissues. Alternatively, the pathogen may act indirectly by inhibiting RuBisCO activase (*Rca*). *Rca* allows the activation of RuBisCO by facilitating the ATP-dependent removal of several inhibitory sugar phosphates from the RuBisCO activase site. This action is necessary for the spontaneous carbamylation of RuBisCO active sites *in vivo* and is thus essential for photosynthetic CO_2 assimilation. According to our results, *RcaA2* expression tends to increase at 6 hpi with normalized relative expression values shifting from 0.9 to ca. 1.5 (Suppl. Table 1).

Sucrose is the end product of photosynthesis and is transported from source to sink tissues. Sucrose catabolism implies the following main enzymes: invertase (INV) catalyzing the irreversible hydrolysis of sucrose into its hexose monomers (Stein and Granot, 2019) and sucrose synthase (SUS) catalyzing the reversible transformation of sucrose and nucleotide diphosphate (NDP) into nucleotide diphosphate glucose (NDP-glucose) and fructose. During plant-fungal pathogen interaction, *SUS* expression was induced in *Arabidopsis* roots infected with *Plasmodiophora brassicae* (Siemens et al., 2006). Under stress conditions, sucrose functions as messenger resulting in the activation of signaling enzymes such as mitogen-activated protein kinases (MAPKs). *SUS* expression is associated with the response of plants to various environmental stresses. According to Figure 2, *SUS2* is slightly over-expressed in the presence of *D. teres* compared to the control condition. Barrero-Sicilia and collaborators (2011) have demonstrated that the expression of genes encoding SUS from barley is modulated by different abiotic stimuli, including water deprivation and cold temperature.

In the previous paragraphs, the gene expression analysis highlighted the impact of *D. teres* in barley (Figure 3). We then aimed at providing an answer to the following question: are there similar or different effects during PsJN or strain B25 application with or without pathogen? We will hereafter present the results relative to the bacterization with PsJN first and then with strain B25 for each studied gene.

Classified as an endochitinase III, *PR8* breaks down the fungal cell wall, resulting in cell lysis and death (Singla et al., 2020). Our results show no modulation in *PR8* expression when barley is bacterized with PsJN at 6 hpi and 12 hpi with normalized relative expression values close to 0.95 and 1.36, respectively (Suppl. Table 1). In addition, the expression of *PR8* does not vary in barley bacterized by strain B25. Other results have shown the modulation of the expression of this gene during a plant-pathogen interaction. For instance, *PR8* is induced in wheat 6 hpi with *Fusarium graminearum* (Wu et al., 2014). *PR8* is also over-expressed in barley in the presence of the fungal pathogen *Puccinia* sp. (Singla et al., 2020) and *E. graminis* f. sp. *hordei*, the causal agent of powdery mildew (Ignatius et al., 1994). During pathogens' attack, a group of proteins is produced by the infected plant including "Pathogenesis-Related" (PR) proteins. PR proteins accumulate in the infected tissues and protect plants against biotic stress. Classified into 17 families, PR proteins have several functions, including antifungal, glucanase and chitinase activities, thaumatin-like proteins, peroxidases and protease inhibitors, endoprotease, ribonuclease, defensin, thionin, lipid-transfer proteins and oxalate oxidase.

In addition to PR proteins, jasmonic acid signaling molecules are also involved in activating the plant's defenses against pathogens. ROS can damage the lipids and, more particularly, the lipid peroxidation products of unsaturated fatty acids lead to cell membrane damage. For instance, α-linolenic acid draws attention since it represents a substrate for the synthesis of the phytohormone jasmonic acid. This metabolic pathway involves the enzyme allene oxide synthase (AOS) followed by the enzyme allene oxide cyclase (AOC). In our case, the expression of *AOC* tends to increase in the presence of the pathogen *D. teres* compared to the control, with normalized relative expression values close to 0.75 and 0.41 at 48 hpi, respectively. In the same way, *AOC* tends to increase with the pathogen and strain PsJN compared to the control, with normalized relative expression values close to 1.13 and 0.63 at 48 hpi, respectively (Suppl. Table 1). On the contrary, *AOC* expression seems to decrease in the presence of *D. teres* in combination with strain B25 compared to the values of the infected plants at 12 and 48 hpi. In grapevine, the presence of PsJN modulates slightly the *AOC* transcript levels. However, *Botrytis* alone induces a significant increase in *PR5* and *AOC* gene expression levels (Miotto-Vilanova et al., 2016). Grapevine plantlets treated with PsJN show a higher expression of *PR* genes (*PR1*, *PR2* and *PR5*) in response to the pathogen. Therefore, in grapevine, PsJN primes the simultaneous induction of the jasmonic acid-related genes (Miotto-Vilanova et al., 2016). In the presence of the *F. oxysporum* pathogen, *PR1* is induced in tomato and its expression is higher when the plant is not treated with *Pseudomonas chlororaphis* used as biocontrol agent (Kamou et al., 2020).

In the presence of *D. teres* and/ or strain PsJN in barley, the antioxidant enzymes *CAT* and *GSTd2* have a higher expression compared to *SOD* (Figure 2). In addition, these three antioxidant enzymes show no significant variations in the presence of strain B25 and/or in combination with the pathogen.

PAL is the first enzyme in the phenylpropanoid pathway, which synthesizes specialized metabolites from L-phenylalanine, including lignin building blocks, flavonoids and phytoalexins (Peltonen and Karjalainen, 1995; Yadav et al., 2020). The induction of PAL activity is considered as a useful indicator of the activation of defense-related responses. In this study, two isoforms of phenylalanine ammonia lyase (*PAL* and *PAL2*) were studied. According to the heat map hierarchical clustering, *PAL* and *PAL2* show different expression patterns and are thus in different clusters. *PAL2* is

induced not only in the presence of the pathogen alone, but also in barley infected by *D. teres* in combination with strain PsJN (Figure 2). *PAL* shows no significant difference in the presence of strain B25. In contrast, *PAL2* appears to be less expressed in the presence of strain B25 or in combination with *D. teres*, though differences are not statistically significant (Suppl. Table 1). According to Chandrasekaran et al. (2017), *PAL* expression is significantly higher in tomato plantlets bacterized with *Bacillus subtilis* compared to non-bacterized plantlets 72 hpi after inoculation with *Xanthomonas campestris* pv. v*esicatoria*. Similarly, Peltonen and Katjalainen (1995) have demonstrated a two- to five-fold increase in *PAL* transcript level in barley and wheat leaves following infection with *Bipolaris sorokiniana*, a necrotrophic cereal pathogen. There is a strong correlation between an increase in *PAL* transcript level and fungal infections in the *Gramineae*, indicating that the synthesis of phenolic compounds is part of their defense reactions (Peltonen and Karjalainen, 1995). The increase in *PAL* transcript level was reported to restrict the infected area, by inducing lignification (Peltonen and Karjalainen, 1995).

Flavonoids play central roles in plant defense against biological and environmental stresses, such as fungal infection. Stress frequently induces flavonoid biosynthesis in plant tissues. In this study, the expression of genes coding for the two flavonoid biosynthetic enzymes, chalcone synthase *CHS* and flavanone-3'-hydroxylase *F3'H*, is analyzed in barley leaves with or without pathogen and/or PGPR.

CHS is the first enzyme involved in the flavonoid pathway and synthesizes naringenin chalcone from three molecules of malonyl-CoA and one molecule of coumaroyl-CoA. According to Figure 2, *CHS* expression tends to increase with strain PsJN. On the contrary, *CHS* expression tends to decrease with strain B25 without significant differences (Figure 2 and Suppl. Table 1). During pathogens' attack, *Sorghum* leaves change their color from light to dark brown (Mizuno et al., 2016). The tan-colored *Sorghum* plants accumulate relatively higher levels of flavones (apigenin and luteolin) than red/purple ones. Indeed, pigments are accumulated in response to infection with a fungus (Mizuno et al., 2016). Many studies have shown that the expression of *CHS* can be induced in response to viruses, bacteria, fungi, nematodes and other pests attacking plants, resulting in the enhanced production of flavonoids (Dao et al., 2011). In barley, two isoforms of *CHS* are present, *CHS1* and *CHS2*, which are different in terms of their affinity with the hydroxycinnamoyl-CoA substrate (Christensen et al., 1998). The expression of *CHS2* in barley infected by *B. graminis* is strongly induced, while *CHS1* is expressed at very low levels (Christensen et al., 1998).

In the flavonoid pathway, flavonoid 3'-hydroxylase (F3'H) catalyzes the hydroxylation of naringenin and dihydrokaempferol (DHK) at the 3' position and belongs to the CYP75B subfamily in the cytochromes P450-dependent monooxygenase superfamily. Like *CHS*, *F3'H* is induced when barley is infected with *D. teres* alone and also in combination with PsJN at 48 hpi. PsJN can be perceived as a pathogenic agent by barley, which triggers defense mechanisms including flavonoids production and, consequently, induces the genes involved in this metabolic pathway. In addition, *F3'H* expression tends to decrease with strain B25 without significant differences (Figure 2 and Suppl. Table 1).

According to Figure 2, two glucan synthase genes show a similar expression pattern and belong to the same cluster. Our results show that *GSL1* and *GSL3* are induced at 12 hpi with *D. teres*. Their expressions are then repressed at 48 hpi. We expected to observe a decrease in *GSL* expression in infected barley bacterized with strain B25, since this beneficial bacterium limits the development

and the symptoms number of net blotch in barley. However, in the presence of PsJN or strain B25, *GSL1* or *GSL3* expressions do not vary.

Many members of the *GSL* family are involved in callose biosynthesis in specific tissues, at certain developmental stages and under different stress conditions. For instance, β-1,3-D-glucan callose is rapidly synthesized upon microbial attack.

A characteristic of cereals and grasses is the presence of (1,3;1,4)-β-D-glucans in the cell wall (Burton et al., 2011). The biosynthesis of this polymer is catalyzed by the members of three cellulose synthase-like (*CslF*/*H*/*J*) subfamilies. *CslF6* shows a slight increase in expression in the presence of PsJN alone (Figure 2). Additionally, *CslF6* displays a lower expression at 12 hpi in the presence of strain B25 alone or in combination with the pathogen. Indeed, *CslF6* expression decreases in the presence of strain B25 compared to PsJN in infected barley, with normalized relative expression values close to 0.65 and 1.17 at 12 hpi, respectively (Suppl. Table 1). The *Csl* gene family is large and has been divided into subgroups, i.e. *CslA* - *CslH*. *HvCslF6* was shown to be directly involved in (1,3;1,4)-β-D-glucan biosynthesis. For instance, the over-expression of *HvCslF6* in transgenic barley resulted in an increase in (1,3;1,4)-β-D-glucan content by more than 40 % in the grain, with even larger increases in vegetative tissues (Burton et al., 2011). The cell wall is a dynamic and complex structure involved in interactions between plants and their environment, notably to limit the further spread of pathogens. According to the results obtained, in the presence of *D. teres*, a barley plant bacterized with strain B25 shows a decreased expression of these genes related to cell wall synthesis.

The role of carbohydrates is well known in the activation of defense mechanisms against pathogens of any kind in plants. However, little information is available concerning the response of plants to beneficial bacteria and in the presence of the pathogen in terms of carbon metabolism. The ability of some beneficial bacteria to improve stress tolerance in different plants by regulating the expression of genes involved in carbohydrate metabolism has been shown (Miotto-Vilanova et al., 2016; Su et al., 2015; Riva and Ribaudo, 2020). According to the results obtained in this study, PsJN does not modulate the expression of the selected genes. On the contrary, strain B25 slightly decreases the expression of *RcaA2* and *SUS2* (Suppl. Table 1). In other studies, strain PsJN, modulates the carbohydrate metabolism-related genes and thus increases cold tolerance in grapevine (Miotto-Vilanova et al., 2016; Su et al., 2015). In addition, *Pseudomonas pseudoalcaligenes* changes both the sugar metabolism and the plant defense, leading to an improved tolerance against *Sclerotium rolfsii* in tomato (Riva and Ribaudo, 2020). These results may indicate that bacteria manipulate the expression of defense genes to ensure the establishment of an alert state, thus enabling an efficient and quick response to pathogens.

In our study, PsJN was used as a “bacterization control” since this strain has no effect on the development of the agent responsible for net blotch. Therefore, we can hypothesize that PsJN can induce defense mechanisms in the plant by increasing gene expression without limiting the growth of *D. teres* and without reducing stress symptoms on barley leaves. These results can be explained by the fact that the beneficial bacteria are initially recognized as plant pathogens and, therefore, they elicit the expression of defense-related genes (Kamou et al., 2020).

With strain B25, the expression of some genes shows a tendency towards repression compared to the control (Figure 3). We may therefore infer that strain B25 does not protect barley trough the induction of defense-related genes since their expression decreases. However, strain B25

may protect its host plant by implementing one of two possible mechanisms: firstly, the strain could produce a biofilm preventing the pathogen from accessing the barley cell wall; secondly, strain B25 could secrete antifungal molecules that might stop the development of the pathogen. These hypotheses must be checked with future experiments.

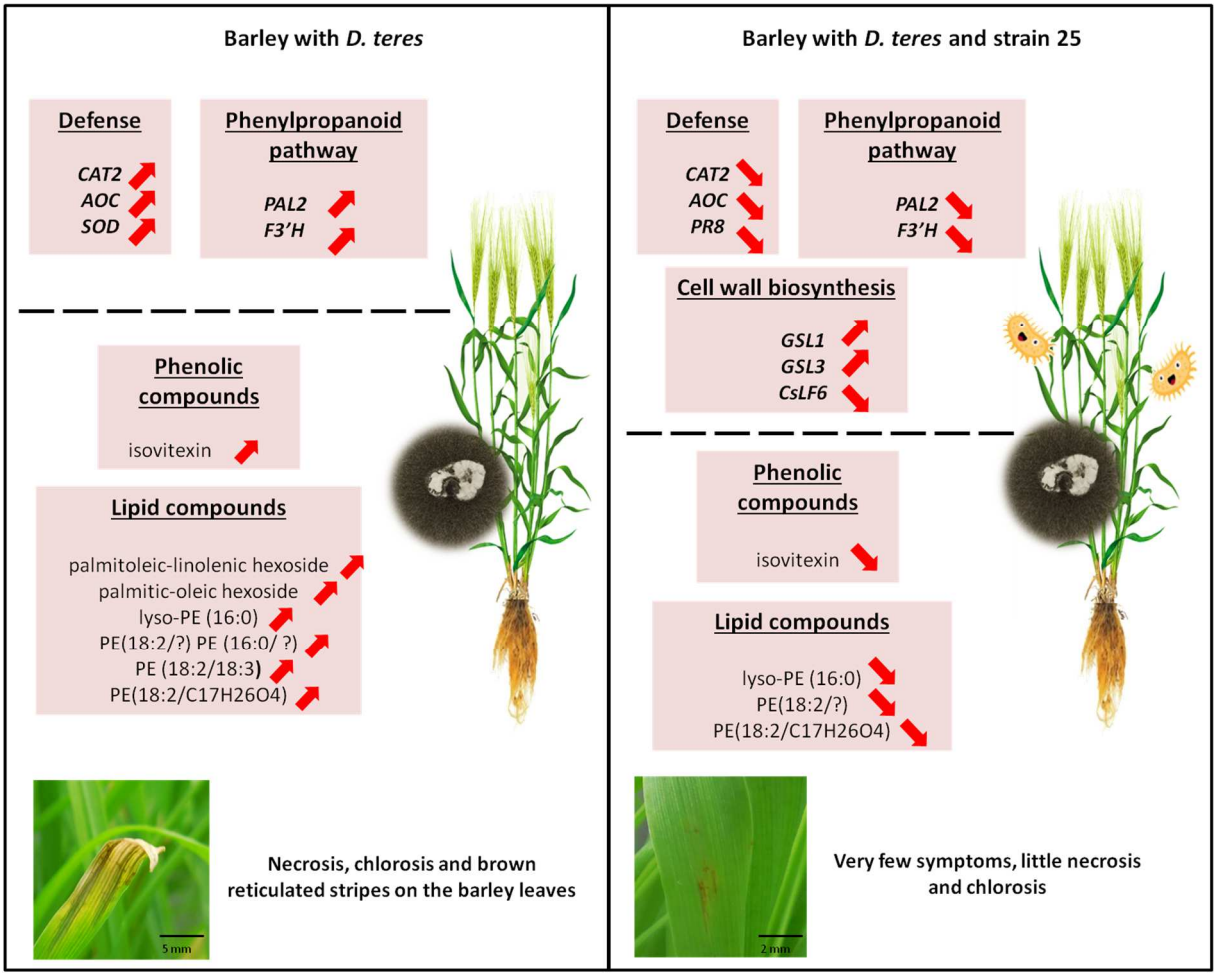

Figure 3. Schematic overview representing the impact of *D. teres* in the absence and presence of strain B25 on barley leaves. In the presence of the fungus alone, barley induces the expression of genes related to defense response and the phenylpropanoid pathway. In the context of biological control, strain B25 acts as an antagonist of *D. teres*.

When comparing the data obtained for PsJN and strain B25, results are very distinct. This difference can be explained by their antagonistic effects against net blotch. Indeed, barley plants infected with *D. teres* and bacterized with PsJN showed similar symptom levels as those infected only with *D. teres*. In contrast, plants infected and bacterized with strain B25 had a lower number of symptoms on the leaves. This decrease in the number of brown spots has great importance on the primary and secondary metabolisms of barley. For instance, a barley leaf with symptoms develops more defense mechanisms. In addition, the reduction in healthy leaf area has a direct impact on photosynthetic performance and carbohydrate assimilation.

3.3. Untargeted metabolomics on barley leaves infected by *D. teres* in the absence/ presence of PGPR

Our objective was to conduct a combined gene expression and metabolomic analysis to gain information concerning the biological mechanism underlying the increased defense to net blotch in the presence of beneficial bacteria. An untargeted metabolomics study was performed using the same samples as for RT-qPCR analysis. Time-points 12 h and 48 h were selected based on the results obtained by RT-qPCR. Indeed, gene expression shows more differences at 12 hpi and 48 hpi and, therefore, significant differences could also be observed in the accumulation of metabolites. The goal was to enrich and complement the gene expression data and to attempt to identify metabolites spotted as differentially abundant between modalities during the tripartite interaction barley - *D. teres* - PGPR. According to the results obtained, barley produces different metabolites in the presence of the pathogen with/without bacteria while 12 hpi is the time-point where the differences between modalities are the most significant (Table 2). Metabolomics results are consistent with RT-qPCR results, 12 hpi also being the time-point at which several genes related to defense, the phenylpropanoid pathway and cell wall biosynthesis are over-expressed in all the experimental conditions.

In total, 25 metabolites were putatively identified among the differentially abundant ones according to the experimental conditions. The identified metabolites belong mainly to the following categories: nucleotides, phenolic compounds, fatty acyls (FA) and glycerophospholipids (PL) (Table 2).

Among the phenolic compounds, the first identified metabolite is galloyl glucose (n° 2). This compound plays a role in cell wall thickening and also as a phytoalexin. Our results show that galloyl glucose is present in higher abundance in barley leaves bacterized with strain B25 at 48 hpi compared to control plants (Table 2).

N-*p*-coumaroylhydroxydehydroagmatine (n° 3, 5 and 7) and *N*-*p*-coumaroylhydroxyagmatine (n° 4 and 6) are hydroxycinnamic acid amides found in cereals. These compounds are present at higher levels in barley leaves infected with *D. teres* and bacterized with PsJN at 12 hpi compared to barley leaves infected solely with *D. teres* at the same time-point (Table 2). A peroxidase catalyzes the reaction to obtain hordatine from *p*-hydroxycinnamoylagmatine. Hordatines, as well as *p*-coumaroylagmatine and its hydroxylated form, act as preformed defense compounds in barley grains or as inducible defense compounds at the onset of pathogens' attack in barley plants. Hordatin A is a dimer of *p*-coumaroylagmatine, while hordatin B is a conjugate analogous to *p*-coumaroyl and feruloylagmatins. According to the results obtained with RT-qPCR, *AOC* expression tends to increase in the presence of the pathogen and in combination with PsJN strain compared with control at 12 hpi (Figure 2). We can therefore hypothesize that *AOC* induction increases JA production, leading to an increase of *N*-*p*-coumaroylhydroxyagmatine.

The third identified phenolic compound is isovitexin (n° 8), a C-glycosylated flavone belonging to the phenylpropanoid pathway. Previous studies have demonstrated that barley leaves contain a large number of flavonoids including C-glycosylated flavones, isovitexin-7-*O*-glucoside (saponarin) and isoorientin-7-*O*-glucoside (lutonarin). In our study, isovitexin abundance is higher in pathogen-free and bacteria-free leaves at 12 hpi compared with leaves bacterized only with strain B25 at the same time-point (Table 2).

Table 2. List of the compounds identified in barley leaves infected by *D. teres*, in combination with PsJN or strain B25, using UHPLC-DAD-ESI-MS/MS analysis. Metabolites were annotated/ identified based on exact mass, retention time, MS2 fragmentation pattern and UV-visible spectrum by comparison with data in databases and/or literature. The abbreviation of the names of the molecules classes is inspired by LIPID MAPS including fatty acyls (FA) –glycerolipid (GL)- -glycerophospholipids (PL)- glycerophosphoethanolamines (PE)- glycerophosphocholines (PC)- glycerophosphoglycerol (PG)

No	RT (min)	Observed m/z	Adduct	Comparison n°	Class	Name	Molecular formula	Theoretical m/z	Mass error (ppm)	MS/MS fragments	Λ max (nm)	Highest mean	Lowest mean	Max fold change	Reference	Data bank reference [a]	MSI level [b]
1	1.23	348.0688	$[M+H]^+$	8	nucleotides	adenosine 3'-monophosphate	$C_{10}H_{14}N_5O_7P$	348.0703	-4.64	**136.0607**, 119.0337, 85.0277, 164.9924, 213.0137	260	Infected T12	Strain B25 infected T12	2.08	/	MID 63401 CID 41211	2
2	2.56	331.0659	$[M-H]^-$	9	phenolic compounds	galloyl glucose	$C_{13}H_{16}O_{10}$	331.0671	-3.54	**168.0058**, **149.9946**, **125.0241**, 124.0156, 331.0668, 123.0082, 313.0553	204 255 320	Strain B25 T48	Control T48	2.03	[1] [2]	CID 124021 MoNA PM011302	2
3	4.60	291.1438	$[M+H]^+$	12	phenolic compounds	N-p-coumaroylhydroxy-dehydroagmatine	$C_{14}H_{18}O_3N_4$	291.1452	-4.70	**147.0452**, **127.0986**, 255.1253, 273.1370, 213.1038, 119.0499, 91.0550, 110.0722	193 206 282	Strain PsJN infected T12	Infected T12	2.27	[3]	/	2
	4.62	289.1298	$[M-H]^-$	12	phenolic compounds	N-p-coumaroylhydroxy-dehydroagmatine	$C_{14}H_{18}O_3N_4$	289.1306	-2.84	**119.0503**	222 283	Strain PsJN infected T12	Infected T12	3.78	[3]	/	2
4	4.62	291.1458	$[M-H]^-$	12	phenolic compounds	N-p-coumaroylhydroxy-agmatine	$C_{14}H_{20}O_3N_4$	291.1463	-1.72	**119.0482**, 208.8628, 226.8755	222 283	Strain PsJN infected T12	Infected T12	2.27	[3]	/	2
5	9.14	291.1446 *	$[M+H]^+$	9	phenolic compounds	N-p-coumaroylhydroxy-dehydroagmatine	$C_{14}H_{18}O_3N_4$	291.1452	-1.96	**147.0437**, 127.0972, 213.1016, 119.0487, 255.1239, 273.1344, 91.0537, 110.0703, 126.0891, 153.0768	216 291 311(sh)	Strain B25 T48	Control T48	2.67	[3]	/	2
	9.14	291.1461 *	$[M+H]^+$	12	phenolic compounds	N-p-coumaroylhydroxy-dehydroagmatine	$C_{14}H_{18}O_3N_4$	291.1452	3.19	**147.0448**, 255.1258, 127.0981, 273.1359, 213.1034, 119.0498, 91.0545, 110.0717, 126.0900, 153.0774	218 291	Strain PsJN infected T12	Infected T12	3.43	[3]	/	2
6	9.21	291.1457	$[M-H]^-$	12	phenolic compounds	N-p-coumaroylhydroxy-agmatine	$C_{14}H_{20}O_3N_4$	291.1463	-2.07	**119.0498**, 208.8656, 226.8741, 100.9340, 150.9163, 132.9036	218 289	Strain PsJN infected T12	Infected T12	2.95	[3]	/	2
7	9.29	289.1297	$[M-H]^-$	12	phenolic compounds	N-p-coumaroylhydroxy-dehydroagmatine	$C_{14}H_{18}O_3N_4$	289.1306	-3.31	**119.0499**	218 289	Strain PsJN infected T12	Infected T12	5.31	[3]	/	2
8	22.66	431.0962	$[M-H]^-$	7	phenolic compounds	isovitexin	$C_{21}H_{20}O_{10}$	431.0984	-4.96	**311.0556**, **283.0638**, 281.0431, 269.0501, 323.0572, 341.0638	214 339 271	Control T12	Strain B25 T12	2.05	[3]	MID 263495	2

Table 2. (Continued)

No	RT (min)	Observed m/z	Adduct	Comparison n°	Class	Putative name	Molecular formula	Theoretical m/z	Mass error (ppm)	MS/MS fragments	Λ max (nm)	Highest mean	Lowest mean	Max fold change	Reference	Data bank reference [a]	MSI level [b]
9	31.99	223.1337	$[M-H]^-$	14	FA	13-oxo-9,11-tridecadienoic acid	$C_{13}H_{20}O_3$	223.1340	-1.23	**223.1330**, **195.1395**, **69.0362**, 59.0154, 179.1451, 167.1112, 153.0937, 161.1324, 205.1224	221	Strain PsJN infected T48	Infected T48	11.52	[4]	CID 11106999 MoNA PR309071	2
10	37.89	518.3221	$[M+H]^+$	7	PL	lyso-PC(18:3)	$C_{26}H_{48}NO_7P$	518.3241	-3.93	**184.0771**, 86.0980, 125.0014, 166.0642, 60.0824, 335.2580, 500.3154, 258.1111, 261.2221	198 221	Strain B25 T12	Control T12	3.81	[5]	CHEBI 133456 LMGP01050038	2
	37.89	518.3221	$[M+H]^+$	11	PL	lyso-PC(18:3)	$C_{26}H_{48}NO_7P$	518.3241	-3.93	**184.0743**, 124.9979, 86.0948, 60.0813, 98.9845, 166.0634, 71.0732, 104.1070, 500.3091, 335.2589, 258.1141	198 221	Strain PsJN T12	Control T12	4.78	[5]	CHEBI 133456 LMGP01050038	2
11	38.11	721.3649	$[M-H]^-$	7	di-fatty acid hexoside	palmitoleic-linolenic hexoside	$C_{34}H_{58}O_{16}$	721.3652	-0.48	**277.2179**, 59.0141, 89.0244, 101.0244, 113.0242, 119.0344, 397.1344, 235.0820, 161.0451, 415.1456, 179.0555	198 221	Control T12	Strain B25 T12	2.27	[6]	/	4
12	38.71	520.3375	$[M+H]^+$	7	PL	lyso-PC(18:2)	$C_{26}H_{50}NO_7P$	520.3398	-4.43	**184.0753**, 86.0979, 125.0009, 166.0638, 60.0821, 71.0742, 98.9857	200 222	Strain B25 T12	Control T12	3.34	[5]	CHEBI 28733 LMGP01050035	2
	38.71	520.3375	$[M+H]^+$	11	PL	lyso-PC(18:2)	$C_{26}H_{50}NO_7P$	520.3398	-4.43	**184.0745**, 124.9986, 86.0953, 60.0816, 166.0627, 71.0733, 98.9844, 104.1069, 337.2717, 502.3261, 258.1070, 520.3314	200 222	Strain PsJN T12	Control T12	4.30	[5]	CHEBI 28733 LMGP01050035	2
13	39.46	699.3802	$[M-H]^-$	7	di-fatty acid hexoside	palmitic-oleic hexoside	$C_{32}H_{60}O_{16}$	699.3809	-1.01	**255.2329**, 59.0139, 89.0242, 101.0235, 119.0349, 397.1336, 71.0139, 235.0819, 415.1450, 279.2333	222	Control T12	Strain B25 T12	2.58	[6]	/	4
	39.46	699.3802	$[M-H]^-$	11	di-fatty acid hexoside	palmitic-oleic hexoside	$C_{32}H_{60}O_{16}$	699.3809	-1.01	**255.2329**, 59.0139, 89.0242, 101.0235, 119.0349, 397.1336, 71.0139, 235.0819, 415.1450, 279.2333	222	Control T12	Strain PsJN T12	2.30	[6]	/	4
	39.46	699.3802	$[M-H]^-$	13	di-fatty acid hexoside	palmitic-oleic hexoside	$C_{32}H_{60}O_{16}$	699.3809	-1.01	**255.2310**, 59.0136, 89.0237, 101.0228, 119.0336, 71.0130, 235.0810, 397.1319, 125.0242, 415.1416, 161.0436	222	Strain PsJN T48	Control T48	2.01	[6]	/	4
14	39.50	452.2771	$[M-H]^-$	7	PL	lyso-PE(16:0)	$C_{21}H_{44}NO_7P$	452.2783	-2.58	**255.2333**, 78.9593, 140.0119, 196.0376	222	Control T12	Strain B25 T12	2.27	/	MID 40776 LMGP02050002 CHEBI 73134 NIST 53862-35-4	2
	39.50	452.2771	$[M-H]^-$	13	PL	lyso-PE(16:0)	$C_{21}H_{44}NO_7P$	452.2783	-2.58	**255.2321**, 78.8588, 140.0109, 196.0367	222	Strain PsJN T48	Control T48	2.09	/	MID 40776 LMGP02050002 CHEBI 73134 NIST 53862-35-4	2

Table 2. (Continued)

No	RT (min)	Observed m/z	Adduct	Comparison n°	Class	Putative name	Molecular formula	Theoretical m/z	Mass error (ppm)	MS/MS fragments	Λ max (nm)	Highest mean	Lowest mean	Max fold change	Reference	Data bank reference [a]	MSI level [b]
15	39.58	355.2828	$[M+H]^+$	7	GL	octadecadienoyl-glycerol	$C_{21}H_{38}O_4$	355.2843	-4.33	**67.0558**, **95.0873**, **81.0719**, 109.1025, 55.0561, 133.1035, 121.1003, 263.2386, 245.2264, 161.1341, 337.2731, 355.2461	223	Strain B25 T12	Control T12	2.21	/	CHEBI 75457 MID 63032 and 45151	2
	39.58	355.2828	$[M+H]^+$	9	GL	octadecadienoyl-glycerol	$C_{21}H_{38}O_4$	355.2843	-4.33	**81.0681**, **67.0535**, **95.0857**, 79.0532, 55.0532, 69.0689, 147.1156, 133.0995, 109.0989, 161.1300	223	Control T48	Strain B25 T48	2.21	/	CHEBI 75457 MID 63032 and 45151	2
	39.58	355.2828	$[M+H]^+$	11	GL	octadecadienoyl-glycerol	$C_{21}H_{38}O_4$	355.2843	-4.33	**81.0708**, **67.0550**, **95.0860**, 109.1011, 263.2339, 135.1172, 123.1169, 161.1312, 147.1195, 175.1468, 337.2747, 245.2274	222	Strain PsJN T12	Control T12	2.42	/	CHEBI 75457 MID 63032 and 45151	2
16	41.24	279.2312	$[M+H]^+$	7	FA	octadecatrienoic acid derivative	$C_{18}H_{30}O_2$	279.2319	-2.41	**81.0691**, **67.0536**, **95.0839**, **149.0221**, 109.0988, 201.0456, 55.0541, 79.0534, 93.06778, 131.0843	223	Strain B25 T12	Control T12	2.41	/	CHEBI 25633	3
17	41.39	676.4167	$[M-H]^-$	7	PL	PE(18:2/?)	/	/	/	**279.2333**, 199.1334, 140.0120, 78.9592, 96.9698, 171.1390, 196.0378, 122.0012, 211.1337, 476.2727, 476.2892, 458.2592, 458.2744, 613.3834	223	Control T12	Strain B25 T12	3.04	/	/	4
18	41.75	1273.8553	$[2M-H]^-$	11	PL	PE(16:0/ ?)	/	/	/	**201.1497**, 255.2338, 636.4292	223	Control T12	Strain PsJN T12	4.36	/	/	4
19	41.87	712.4896	$[M-H]^-$	14	PL	PE(16:0/18:3)	$C_{39}H_{72}NO_8P$	712.4923	-3.70	**277.2184**, **255.2334**, 140.0118, 196.0387, 669.1875, 452.2789	224	Strain PsJN infected T48	Infected T48	2.64	[7]	LMGP02010041	2
20	42.90	752.4500	$[M-H]^-$	7	PL	PE(18:2/C17H26O4)	$C_{40}H_{68}NO_{10}P$	752.4508	-1.10	**293.1752**, **279.2321**, 249.1854, 275.1643, 140.0109, 196.0388, 295.2285, 476.2742, 78.9527	224	Control T12	Strain B25 T12	2.62	[7]	/	3
21	43.88	743.4812	$[M+H]^+$	13	PL	PG(34:4)	$C_{40}H_{71}O_{10}P$	743.4858	-6.11	**571.4733**, **93.0712**, **69.0709**, **95.0874**, 107.0874, 311.2604, 335.2555, 149.1307, 184.0721, 261.2231	224	Strain PsJN T48	Control T48	2.12	/	LMGP04010213	2
22	44.67	728.5181	$[M+H]^+$	11	PL	PC(32:3)	$C_{40}H_{74}NO_8P$	728.5225	-6.00	**184.0741**, 86.0967, 125.0000, 60.0814, 166.0626, 98.9842, 71.0736, 104.1073, 468.3160, 450.2932, 285.2388, 500.3053, 545.4532	225	Strain PsJN T12	Control T12	2.40	/	CHEBI 66847 LMGP01010497	2
23	45.05	736.4910	$[M-H]^-$	11	PL	PE(18:2/18:3)	$C_{41}H_{72}NO_8P$	736.4923	-1.76	**279.2358**, **277.2207**, 140.0129, 196.0392, 78.9601	225	Control T12	Strain PsJN T12	3.24	[7]	LMGP02010665	2

Table 2. (Continued)

No	RT (min)	Observed m/z	Adduct	Comparison n°	Class	Putative name	Molecular formula	Theoretical m/z	Mass error (ppm)	MS/MS fragments	Λ max (nm)	Highest mean	Lowest mean	Max fold change	Reference	Data bank reference [a]	MSI level [b]
24	45.50	756.5505	$[M+H]^+$	11	PL	PC(16:0/18:3)	$C_{42}H_{78}NO_8P$	756.5538	-4.37	**184.0730**, 86.0965, 124.9996, 478.3229, 496.3379, 500.3032, 756.5511	225	Strain PsJN T12	Control T12	4.91	/	CHEBI 84786 LMGP01010598 LMGP01010601	2
25	46.54	449.3403	$[M-H]^-$	13	phyllo-quinones	phylloquinone	$C_{31}H_{46}O_2$	449.3425	-4.85	**434.3195**, 238.0983, 223.0771, 449.3442, 185.0609, 209.0614, 237.0918, 171.0460, 339.2018	225	Strain PsJN T48	Control T48	3.11	[8]	/	3

The comparisons shown in the table are differentially abundant (*p*-value < 0.05 and max fold change > 1.5) in the two experimental conditions of the considered comparisons. Ions in bold are above 50 % relative abundance in MS2. The asterisk (*) indicates that the quantification of compound 5 was made on *m/z* 273.1340 ($[M+H-H_2O]^+$), sh: shoulder.

[1] Tang et al., 2019, Foods MDPI (DOI: 10.3390/foods9010007), [2] Nowicka et al., 2019, Foods Chemistry (DOI: 10.1016/j.foodchem.2018.07.015), [3] Piasecka et al., 2015, Journal of Mass Spectrometry (DOI: 10.1002/jms.3557), [4] Gardner, 1998, Lipids (DOI:10.1007/s11745-998-0265-z), [5] Cho et al., 2012, Journal of Agriculture and Food Chemistry (DOI: 10.10121/jf303702j), [6] Pierson et al., 2014, Food Chemistry (DOI: 10.1016/j.foodchem.2013.10.108), [7] Pi et al., 2016, Analytical Methods (DOI:10.1039/C5AY00776C), [8] Catinot et al., 2008, FEBS Letters (DOI: 10.1016/j.febslet.2007.12.039).

[a] Metlin ID: MID*, PubChem ID: CID*, Lipid Maps: ID: LMGP*, Chemical Entities of Biological Interest (ChEBI) ID: CHEBI*, National Institute of Standards and Technology (NIST) ID: NIST*, MassBank of North America (MoNA) ID: MoNA*.

[b] Metabolite identification level according to Metabolite Standards Initiative recommendation (1- identified metabolites, 2- putatively annotated compounds, 3-putatively characterized compound classes, 4- unknown compounds) (Dunn et al., 2013; Sumner et al., 2007).

The synthesis of isovitexin involves several enzymes, including *CHS* and *F3'H* in the phenylpropanoid pathway. The gene expression results show a decrease in *F3'H* expression in the presence of strain B25, in combination or not with the pathogen (Figure 2). Therefore, it is possible to relate a repression of *CHS* and *F3'H* genes with a decrease in the amount of isovitexin in barley leaves.

For two compounds (n° 11 and 13), the data comprising the exact mass and retention time obtained are similar to those provided by Pierson et al. (2014). However, from the formula given by Pierson and collaborators, we are unable to find the structure of these compounds identified as palmitoleic-linolenic hexoside (n° 11) and palmitic-oleic hexoside (n° 13) (Pierson et al., 2014). For this reason, the MSI level assigned to these two compounds is 4.

Compound n° 25 was identified as phylloquinone. Known as vitamin K1, phylloquinone belongs to the quinone lipids containing a methylated naphtoquinone ring structure and differs in the aliphatic side chain linked to position 3. Phylloquinones are up to three times more abundant in PsJN-bacterized leaves at 48 hpi compared to control ones at the same time-point.

The other identified compounds are all classified as lipids, more precisely two fatty acids or derivatives (n° 9 and 16), one glycerolipid (n° 15) and eleven glycerophospholipids (PL). A fatty acid, more precisely, an oxo-tridecadienoic acid (n° 9) is up to 11.52 times more abundant in barley with strain B25 at 12 hpi compared to non-infected barley leaves at the same time-point (Table 2).

Based on their molecular structures, lipids can be classified as polar and non-polar. Non-polar lipids include triacylglycerols, sterols and tocopherols. Glycerophospholipids are the most prominent members of polar lipids. Among the glycerophospholipids identified in this study, six compounds are glycerophosphoethanolamines (PE) (n° 14, 17, 18, 19, 20 and 23), four are glycerophosphocholines (PC) (n° 10, 12, 22 and 24), and one is a glycerophosphoglycerol (PG) (n° 21). According to the results obtained, barley leaves in the presence of strain B25 show lower levels of lyso-PE(16:0) and PE(18:2/C17H26O4) at 12 hpi compared to control plants (Table 2 and Figure 3). On the contrary, the relative abundance of other unsaturated species, such as PE(16:0/18:3) and PE(18:2/ 18:3) increases in barley with strain PsJN and *D. teres* at 48 hpi or decreases with PsJN without *D. teres* at 12 hpi, respectively (Figure 3). The regulation of the glycerolipids is important in plants to maintain membrane fluidity and integrity under stress conditions. Lipids also play an important role in the plant's defense response. When exposed to many types of (a)biotic stress, plants sense these exogenous stimuli and transmit the signal through the plasma membrane. The change of the phospholipid composition was studied during the interaction between barley and *Fusarium*. Indeed, the levels of phosphatidylcholine PC(36:4) increased, while lysophosphatidylcholine lyso-PC(16:0), lyso-PC(18:2) and lyso-PC(18:3) decreased in abundance (Reyna et al., 2019).

In this study, an untargeted metabolomics analysis identified mainly phenolic compounds and lipids, two classes of compounds known to undergo changes in abundance due to biotic stress. Indeed, flavonoids are molecules produced in response to biotic stress, thus their properties and applications have attracted growing interest. At the same time, lipids are known to be involved in intracellular signaling upon pathogens' attack including virus, bacteria, fungi, nematodes and other biotic stressors. The present results also show the potential protection of strain B25 against net blotch. The presence of *D. teres* and the beneficial bacteria implies changes in the production of metabolites in barley. Lipid compounds are more abundant in plants infected with net blotch. In addition, barley tends to produce fewer defense compounds in the presence of strain B25. A

difference in the production of metabolites was also observed when comparing barley plants bacterized by PsJN and strain B25. These differences in transcripts levels and metabolites seem to be correlated to their difference in antagonistic effect towards *D. teres*.

Conclusions and future perspectives

In summary, the infection with *D. teres* causes significant transcriptional and metabolomic changes in barley. The research presented here highlights the molecular changes caused by beneficial PGPR used as biocontrol agents in agriculture. Strain B25 is able to protect barley against net blotch. Additionally, the expression of genes involved in stress response is mitigated and fewer compounds involved in defense mechanisms are produced. These results are likely related to the cultivar used. Future studies, using other cultivars, will validate these results and contribute to identify new markers of susceptibility or tolerance to the disease. The gene expression study and the relative quantification of metabolites performed here represent, to our knowledge, the first study on the tripartite interaction among barley, the biocontrol agent strain B25 and *D. teres*, the pathogen causing barley net blotch.

Acknowledgments: This work was supported by grand-Reims and Grand-Est region. The authors gratefully acknowledge BAYER SAS Lyon for providing the *D. teres* HE 019, and more specifically Marie-Pascale Latorse, Stéphane Brunet and Catherine Wantier for their technical assistance and participation in this study.

Author Contributions: A.B., S.C. and G.G. performed the experiments. A.B., S.C. and G.G. analyzed the data and prepared the figures and tables. E.A.B., C.J. and G.G. conceived the experiments. S.C., G.G., S.P., Q.E., K.S., J-F.H. and J.R. provided feedback on the draft and on the interpretation of the data. E.A.B. and C.J. managed the project. All authors read and approved the final draft.

Funding: This research did not receive any external funding.

Bibliography

Arabi, M.I.E., Alek, H., Jawhar, M., Al-Shehadah, E., 2020. Expression of PAL and PR2 pathogenesis related genes in barley plants challenged with closely related *Pyrenophora* species. Cereal Res. Commun. 48, 211–216. https://doi.org/10.1007/s42976-020-00033-0.

Backes, A., Guerriero, G., Ait Barka, E., Jacquard, C., 2021a. *Pyrenophora teres*: taxonomy, morphology, interaction with barley, and mode of control. Front. in Plant Sci. 12, 1-18. https://doi.org/10.3389/fpls.2021.614951.

Backes, A., Hausman, J.-F., Renaut, J., Ait Barka, E., Jacquard, C., Guerriero, G., 2020. Expression analysis of cell wall-Related genes in the plant pathogenic fungus *Drechslera teres*. Genes 11, 1–17. https://doi.org/10.3390/genes11030300.

Backes, A., Vaillant-Gaveau, N., Esmaeel, Q., Ait Barka, E., Jacquard, C., 2021b. A biological agent modulates the physiology of barley infected with *Drechslera teres*. Scientific Reports 11, 1-16. http://doi.org/ 10.1038/s41598-021-87853-0.

Barrero-Sicilia, C., Hernando-Amado, S., González-Melendi, P., Carbonero, P., 2011. Structure, expression profile and subcellular localisation of four different sucrose synthase genes from barley. Planta 234, 391–403. https://doi.org/10.1007/s00425-011-1408-x.

Burton, R.A., Collins, H.M., Kibble, N.A.J., Smith, J.A., Shirley, N.J., Jobling, S.A., Henderson, M., Singh, R.R., Pettolino, F., Wilson, S.M., Bird, A.R., Topping, D.L., Bacic, A., Fincher, G.B., 2011. Over-expression of specific HvCslF cellulose synthase-like genes in transgenic barley increases the

levels of cell wall (1,3;1,4)-β-d-glucans and alters their fine structure. Plant Biotechnol. J. 9, 117–135. https://doi.org/10.1111/j.1467-7652.2010.00532.x.

Catinot, J., Buchala, A., Abou-Mansour, E., Métraux, J.-P., 2008. Salicylic acid production in response to biotic and abiotic stress depends on isochorismate in *Nicotiana benthamiana*. FEBS Lett. 582, 473–478. https://doi.org/10.1016/j.febslet.2007.12.039.

Chandrasekaran, M., Belachew, S.T., Yoon, E., Chun, S.C., 2017. Expression of β-1,3-glucanase (GLU) and phenylalanine ammonia-lyase (PAL) genes and their enzymes in tomato plants induced after treatment with *Bacillus subtilis* CBR05 against *Xanthomonas campestris* pv. *vesicatoria*. Journal of General Plant Pathology 83, 7-13. http://doi.org/ 10.1007/s10327-016-0692-5.

Cho, K., Kim, Y., Wi, S.J., Seo, J.B., Kwon, J., Chung, J.H., Park, K.Y., Nam, M.H., 2012. Nontargeted metabolite profiling in compatible pathogen-inoculated tobacco (*Nicotiana tabacum* L. cv. Wisconsin 38) using UPLC-Q-TOF/MS. J. Agric. Food Chem. 60, 11015–11028. https://doi.org/10.1021/jf303702j.

Christensen, A.B., Gregersen, P.L., Schröder, J., Collinge, D.B., 1998. A chalcone synthase with an unusual substrate preference is expressed in barley leaves in response to UV light and pathogen attack. Plant Mol. Biol. 37, 849–857. https://doi.org/10.1023/A:1006031822141.

Dao, T.T.H., Linthorst, H.J.M., Verpoorte, R., 2011. Chalcone synthase and its functions in plant resistance. Phytochem. Rev. 10, 397-412. https://doi.org/10.1007/s11101-011-9211-7.

Dunn, W.B., Erban, A., Weber, R.J.M., Creek, D.J., Brown, M., Breitling, R., Hankemeier, T., Goodacre, R., Neumann, S., Kopka, J., Viant, M.R., 2013. Mass appeal: metabolite identification in mass spectrometry-focused untargeted metabolomics. Metabolomics 9, 44–66. https://doi.org/10.1007/s11306-012-0434-4.

Ferdous, J., Li, Y., Reid, N., Langridge, P., Shi, B.-J., Tricker, P.J., 2015. Identification of reference genes for quantitative expression analysis of microRNAs and mRNAs in barley under various stress conditions. PloS One 10, 1-20. https://doi.org/10.1371/journal.pone.0118503.

Gardner, H.W., 1998. 9-Hydroxy-traumatin, a new metabolite of the lipoxygenase pathway. Lipids 33, 745–749. https://doi.org/10.1007/s11745-998-0265-z.

Goel, N., Kumar Paul, P., 2020. *Dreschlera graminae* downregulates Rubisco expression in barley. Arch. Phytopathol. Plant Prot. 53, 540–551. https://doi.org/10.1080/03235408.2020.1762964.

Huang, J., Gu, M., Lai, Z., Fan, B., Shi, K., Zhou, Y.-H., Yu, J.-Q., Chen, Z., 2010. Functional analysis of the *Arabidopsis* PAL gene family in plant growth, development, and response to environmental stress. Plant Physiol. 153, 1526–1538. https://doi.org/10.1104/pp.110.157370.

Ignatius, S.M.J., Chopra, R.K., Muthukrishnan, S., 1994. Effects of fungal infection and wounding on the expression of chitinases and β-1,3glucanases in near-isogenic lines of barley. Physiol. Plant 90, 584–592. https://doi.org/10.1111/j.1399-3054.1994.tb08818.x.

Jannoey, P., Channei, D., Kotcharerk, J., Pongprasert, W., Nomura, M., 2017. Expression analysis of genes related to rice resistance against brown planthopper, *Nilaparvata lugens*. Rice Sci. 24, 163–172. https://doi.org/10.1016/j.rsci.2016.10.001.

Jawhar, M., Al-Shehadah, E., Shoaib, A., Orfi, M., Al-Daoude, A., 2017. Changes in salicylic acid and gene expression levels during barley-*Blumeria Graminis* interaction. J. Plant Pathol. 99, 651–656. https://doi.org/10.4454/jpp.v99i3.3942.

Kamou, N.N., Cazorla, F., Kandylas, G., Lagopodi, A.L., 2020. Induction of defense-related genes in tomato plants after treatments with the biocontrol agents *Pseudomonas chlororaphis* ToZa7 and *Clonostachys rosea* IK726. Arch. Microbiol. 202, 257–267. https://doi.org/10.1007/s00203-019-01739-4.

Khan, S., Rowe, S.C., Harmon, F.G., 2010. Coordination of the maize transcriptome by a conserved circadian clock. BMC Plant Biol. 10, 1-15. https://doi.org/10.1186/1471-2229-10-126.

Lightfoot, D.J., Mcgrann, G.R.D., Able, A.J., 2017. The role of a cytosolic superoxide dismutase in barley–pathogen interactions. Mol. Plant Pathol. 18, 323–335. https://doi.org/10.1111/mpp.12399.

Luna, C.M., Pastori, G.M., Driscoll, S., Groten, K., Bernard, S., Foyer, C.H., 2005. Drought controls on H2O2 accumulation, catalase (CAT) activity and CAT gene expression in wheat. J. Exp. Bot. 56, 417–423. https://doi.org/10.1093/jxb/eri039.

Maucher, H., Stenzel, I., Miersch, O., Stein, N., Prasad, M., Zierold, U., Schweizer, P., Dorer, C., Hause, B., Wasternack, C., 2004. The allene oxide cyclase of barley (*Hordeum vulgare* L.)—cloning and organ-specific expression. Phytochemistry 65, 801–811. https://doi.org/10.1016/j.phytochem.2004.01.009.

Miotto-Vilanova, L., Jacquard, C., Courteaux, B., Wortham, L., Michel, J., Clément, C., Barka, E.A., Sanchez, L., 2016. *Burkholderia phytofirmans* PsJN confers grapevine resistance against *Botrytis cinerea* via a direct antimicrobial effect combined with a better resource mobilization. Front. Plant Sci. 7, 1–15. https://doi.org/10.3389/fpls.2016.01236.

Mizuno, H., Yazawa, T., Kasuga, S., Sawada, Y., Kanamori, H., Ogo, Y., Hirai, M.Y., Matsumoto, T., Kawahigashi, H., 2016. Expression of flavone synthase II and flavonoid 3'-hydroxylase is associated with color variation in tan-colored injured leaves of Sorghum. Front. Plant Sci. 7, 1–10. https://doi.org/10.3389/fpls.2016.01718.

Nowak, J., 1998. Benefits ofin vitro "biotization" of plant tissue cultures with microbial inoculants. Vitro Cell. Dev. Biol. Plant 34, 122–130. https://doi.org/10.1007/BF02822776.

Nowicka, A., Kucharska, A.Z., Sokół-Łętowska, A., Fecka, I., 2019. Comparison of polyphenol content and antioxidant capacity of strawberry fruit from 90 cultivars of *Fragaria* × *ananassa* Duch. Food Chem. 270, 32–46. https://doi.org/10.1016/j.foodchem.2018.07.015.

Peltonen, S., Karjalainen, R., 1995. Phenylalanine ammonia-lyase activity in barley after infection with *Bipolaris sorokiniana* or treatment with its purified xylanase. J. Phytopathol. 143, 239–245. https://doi.org/10.1111/j.1439-0434.1995.tb00606.x.

Pi, J., Wu, X., Feng, Y., 2016. Fragmentation patterns of five types of phospholipids by ultra-high-performance liquid chromatography electrospray ionization quadrupole time-of-flight tandem mass spectrometry. Anal. Methods 8, 1319–1332. https://doi.org/10.1039/C5AY00776C.

Piasecka, A., Sawikowska, A., Krajewski, P., Kachlicki, P., 2015. Combined mass spectrometric and chromatographic methods for in-depth analysis of phenolic secondary metabolites in barley leaves. J. Mass Spectrom. 50, 513–532. https://doi.org/10.1002/jms.3557.

Pierson, J.T., Monteith, G.R., Roberts-Thomson, S.J., Dietzgen, R.G., Gidley, M.J., Shaw, P.N., 2014. Phytochemical extraction, characterisation and comparative distribution across four mango (*Mangifera indica* L.) fruit varieties. Food Chem. 149, 253–263. https://doi.org/10.1016/j.foodchem.2013.10.108.

Prasad, M., Srinivasan, R., Chaudhary, M., Choudhary, M., Jat, L.K., 2019. Chapter Seven - Plant growth promoting rhizobacteria (PGPR) for sustainable agriculture: perspectives and challenges, in: Singh, A.K., Kumar, A., Singh, P.K. (Eds.), PGPR Amelioration in Sustainable Agriculture. Woodhead Publishing, pp. 129–157. https://doi.org/10.1016/B978-0-12-815879-1.00007-0.

Qi, P.-F., Balcerzak, M., Rocheleau, H., Leung, W., Wei, Y.-M., Zheng, Y.-L., Ouellet, T., 2016. Jasmonic acid and abscisic acid play important roles in host–pathogen interaction between *Fusarium graminearum* and wheat during the early stages of fusarium head blight. Physiol. Mol. Plant Pathol. 93, 39–48. https://doi.org/10.1016/j.pmpp.2015.12.004.

Reyna, M., Peppino Margutti, M., Villasuso, A.L., 2019. Lipid profiling of barley root in interaction with *Fusarium macroconidia*. Environ. Exp. Bot. 166, 1-11. https://doi.org/10.1016/j.envexpbot.2019.06.001.

Riva, D.S., Ribaudo, C.M., 2020. Inoculation with *Pseudomonas pseudoalcaligenes* lead to changes in plant sugar metabolism and defense that enhance tolerance against the pathogenic fungus *Sclerotium rolfsii*. Am. Sci. Res. J. Eng. Technol. Sci. ASRJETS 69, 89–104.

Sharma, M., Bhatt, D., 2015. The circadian clock and defence signalling in plants. Mol. Plant Pathol. 16, 210–218. https://doi.org/10.1111/mpp.12178.

Shiraishi, T., Yamada, T., Nicholson, R.L., Kunoh, H., 1995. Phenylalanine ammonia-lyase in barley: activity enhancement in response to *Erysiphe graminis* f.sp. *hordei* (race 1) a pathogen, and *Erysiphe pisi*, a nonpathogen. Physiol. Mol. Plant Pathol. 46, 153–162. https://doi.org/10.1006/pmpp.1995.1012.

Siemens, J., Keller, I., Sarx, J., Kunz, S., Schuller, A., Nagel, W., Schmülling, T., Parniske, M., Ludwig-Müller, J., 2006. Transcriptome analysis of *Arabidopsis* clubroots indicate a key role for cytokinins in disease development. Mol. Plant-Microbe Interactions 19, 480–494. https://doi.org/10.1094/MPMI-19-0480.

Singla, P., Bhardwaj, R.D., Kaur, S., Kaur, J., Grewal, S.K., 2020. Metabolic adjustments during compatible interaction between barley genotypes and stripe rust pathogen. Plant Physiol. Biochem. 147, 295–302. https://doi.org/10.1016/j.plaphy.2019.12.030.

Stein, O., Granot, D., 2019. An overview of sucrose synthases in plants. Front. Plant Sci. 10, 1–14. https://doi.org/10.3389/fpls.2019.00095.

Su, F., Jacquard, C., Villaume, S., Michel, J., Rabenoelina, F., Clément, C., Ait Barka, E., Dhondt-Cordelier, S., Vaillant-Gaveau, N., 2015. *Burkholderia phytofirmans* PsJN reduces impact of freezing temperatures on photosynthesis in *Arabidopsis thaliana*. Front. Plant Sci. 6, 1–13. https://doi.org/10.3389/fpls.2015.00810.

Sumner, L.W., Amberg, A., Barrett, D., Beale, M.H., Beger, R., Daykin, C.A., Fan, T.W.-M., Fiehn, O., Goodacre, R., Griffin, J.L., Hankemeier, T., Hardy, N., Harnly, J., Higashi, R., Kopka, J., Lane, A.N., Lindon, J.C., Marriott, P., Nicholls, A.W., Reily, M.D., Thaden, J.J., Viant, M.R., 2007. Proposed minimum reporting standards for chemical analysis Chemical Analysis Working Group (CAWG) Metabolomics Standards Initiative (MSI). Metabolomics Off. J. Metabolomic Soc. 3, 211–221. https://doi.org/10.1007/s11306-007-0082-2.

Tang, J., Dunshea, F.R., Suleria, H.A.R., 2019. LC-ESI-QTOF/MS characterization of phenolic compounds from medicinal plants (hops and juniper berries) and their antioxidant activity. Foods Basel Switz. 9, 1–25. https://doi.org/10.3390/foods9010007.

Wu, S., Wang, H., Yang, Z., Kong, L., 2014. Expression comparisons of pathogenesis-related (PR) genes in wheat in response to infection/infestation by *Fusarium*, yellow dwarf virus (YDV) aphid-transmitted and Hessian fly. J. Integr. Agric. 13, 926–936. https://doi.org/10.1016/S2095-3119(13)60570-5.

Yadav, V., Wang, Z., Wei, C., Amo, A., Ahmed, B., Yang, X., Zhang, X., 2020. Phenylpropanoid pathway engineering: an emerging approach towards plant defense. Pathogens 9, 1-25. https://doi.org/10.3390/pathogens9040312.